



Available online at www.sciencedirect.com

SCIENCE @ DIRECT®

Optical Fiber Technology 10 (2004) 325–335

Optical Fiber
Technology

www.elsevier.com/locate/yofte

Fabrication of microstructured polymer optical fibres

Geoff Barton^a, Martijn A. van Eijkelenborg^{b,*}, Geoffrey Henry^b,
Maryanne C.J. Large^{b,c}, Joseph Zagari^{a,b}

^a *Department of Chemical Engineering, University of Sydney, NSW 2006, Australia*

^b *Optical Fibre Technology Centre, Australian Photonics Cooperative Research Centre, University of Sydney,
206 National Innovation Centre, Australian Technology Park, Eveleigh, NSW 1430, Australia*

^c *School of Physics, University of Sydney, NSW 2006, Australia*

Received 7 January 2004; revised 3 May 2004

Available online 27 July 2004

Abstract

A methodology is presented suitable for the fabrication of a wide range of microstructured polymer optical fibres (mPOFs), a recent development where light guidance is achieved through the incorporation of a pattern of air channels that run the entire length of the fibre. We show that the key to good mPOF fabrication is a secondary draw oven that has tight control over the length (15–20 mm) and temperature ($\pm 1^\circ\text{C}$) of the hot-zone while maintaining fibre draw tension high enough (50–150 g) to ensure an acceptable level of partial hole collapse (30–40%) due to surface tension effects. Diverse mPOFs with diameters in the range 200–1200 μm have been fabricated with typical standard deviations of 2–3 μm .

© 2004 Elsevier Inc. All rights reserved.

1. Introduction

Microstructured polymer optical fibres (mPOFs) offer the potential for fabricating fibres with an almost limitless range of internal hole structures [1–3]. Along with the relatively low draw temperatures associated with polymers (here PMMA), mPOFs have emerged as a viable alternative to microstructured glass optical fibres for specific applications. The

* Corresponding author. Fax: +61-2-9351-1911.

E-mail address: m.eijkelenborg@ofc.usyd.edu.au (M.A. van Eijkelenborg).

material properties of PMMA provide advantages relative to silica in the fabrication of microstructured optical fibres when it is appreciated that the drawing of all such fibres is governed by the balance between surface tension and viscosity related forces. While the viscosity of PMMA and silica are of similar magnitudes at their respective draw temperatures [4,5], PMMA's surface tension is an order of magnitude lower than that of silica [6,7]. Thus by lowering the draw temperature, and hence increasing both the viscosity and the required draw tension, hole distortion and collapse due to surface tension effects can be minimised allowing fine-scale mPOFs to be drawn. This paper presents a fabrication methodology that exploits these material properties allowing the manufacture of a wide range of mPOFs.

2. Fabrication methodology

The overall mPOF fabrication procedure is summarised in Fig. 1. After designing the structure required in the final fibre (taking into account the expected 30–40% hole collapse

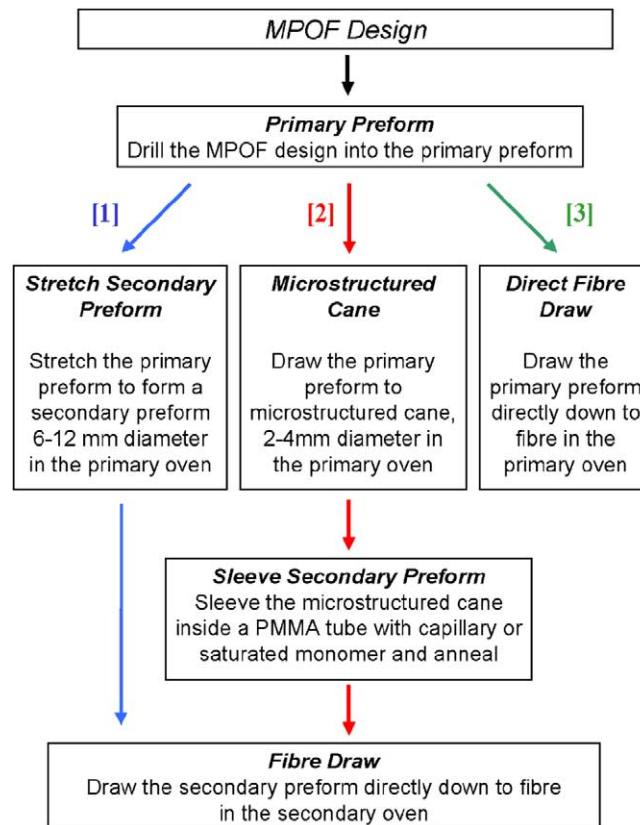


Fig. 1. Schematic of the microstructured polymer fibre fabrication procedure, showing the three main fabrication options.

during fabrication), the hole pattern is drilled into the primary preform using a computer numerical controlled (CNC) mill. The coated drill bits produce deep holes with minimal drill wander while leaving the inside of the holes with a smooth finish, the latter being of importance in that it minimises the likelihood of surface roughness induced scattering in the drawn fibre. Hole sizes at the preform stage are typically 1–10 mm in diameter. At the present time, the finest primary preform structure that can be drilled involves 1 mm holes with 0.1 mm wall thickness between holes to a depth of 65 mm. The longest preform that can currently be drilled is 140 mm in length using 2 mm drills that are 70 mm long with a hole spacing of 2.5 mm. Note that the holes are drilled from both ends of the preform.

Primary preforms can be drawn directly to fibre using a one-stage (i.e., primary oven only) process, although the fibre diameter control is generally poor (at best around $\pm 30 \mu\text{m}$). The main role of the primary oven is thus to produce either a ‘stretched’ secondary preform or a microstructured cane that is subsequently sleeved to form a secondary preform. The alternative employed depends primarily on the dimensions required for the hole structure in the final fibre. For most mPOF designs, the stretched secondary preform is drawn directly to fibre. However, some mPOF designs (such as the small-core fibre described in [8]) require that the final hole sizes be of the order of a micron (or less) and hence the sleeving technique is used. The final step involves drawing the secondary preform to fibre.

The secondary preform (6–12 mm in diameter and at least 15 cm in length) is attached to an extension tube which is in turn attached to the feeder that lowers the preform into the oven where neck-down occurs with the fibre being drawn by a capstan onto a spool. Fibre diameter is measured online using an *Anritsu* KL151A. This laser-based system nominally operates at 1000 Hz but by default employs simple (128 data points) signal averaging giving an effective sampling rate of 7.8 Hz. After diameter measurement, the fibre is guided through a *Check Line* three-wheel tension monitor with a 0–500 g operating range. An acceptable level of partial hole collapse can generally be achieved by maintaining tension in the range 50–150 g by adjusting the oven temperature.

Initially a ‘heat curing’ oven (to cure the polymer coating on silica fibres) was used as the secondary oven for drawing mPOFs. Operated without any feedback control, this produced fibre whose diameter typically varied by up to $\pm 20 \mu\text{m}$. An attempt to use feedback control to reduce this variability by adjusting the draw speed based on the deviation of the measured diameter from the set-point value was largely unsuccessful. As will be discussed, this failure was traced to the size of the ‘hot-zone’ (defined as that region above the PMMA deformation temperature of 145°C) within the oven.

Under steady operating conditions, mass conservation dictates the following relationship between the preform feed rate (v_{feed}) and diameter (D), and the fibre draw speed (v_{draw}) and diameter (d):

$$\frac{D^2}{d^2} = \frac{v_{\text{draw}}}{v_{\text{feed}}}$$

Thus manual control of the fibre diameter should be achievable simply by accurately setting the feed and draw rates for a set preform diameter. The first two rows in Table 1 show experimental results that clearly indicate that even after a considerable length of time, steady operating conditions (in terms of mass conservation) had not been achieved, pre-

Table 1

Comparison of the drawn fibre diameter with that calculated using the mass conservation equation under different fibre draw conditions using the 'heat-curing' secondary oven (first two draws) and the purpose-built secondary oven (last draw)

Preform diameter (mm)	Feed rate (mm/min)	Draw speed (m/min)	Measured fibre diameter (μm)	Calculated fibre diameter (μm)
12.5	10	2	1130	884
12.5	3	3	245	395
8.0	3	4.8	202	200

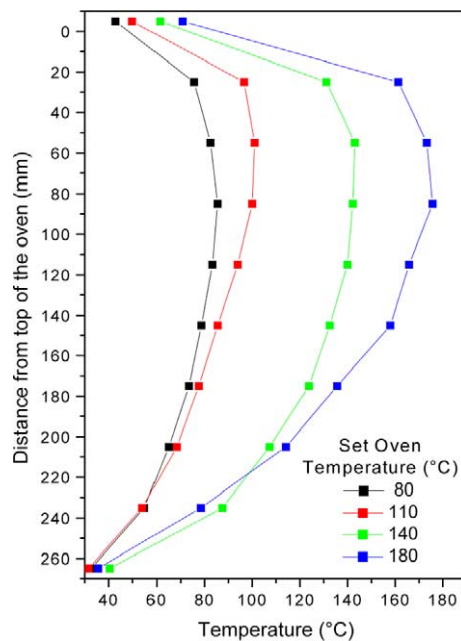


Fig. 2. Oven temperature profiles measured as a function of the distance from the top of the oven, for the initial 'heat-curing' secondary oven. The effective hot-zone is approximately 140 mm long.

sumably due to the slow accumulation (or depletion) of material within the oven hot-zone. This behaviour implies that the neck-down region was slowly moving with time through the hot-zone.

To examine this hypothesis, the temperature profile was measured using thermocouples embedded in a stationary (i.e., not being drawn to fibre) preform. These measurements were made at four nominal oven temperatures and are shown in Fig. 2. Thus at a nominal oven temperature of 180 °C, the hot-zone was approximately 140 mm long, certainly large enough to allow considerable movement of the neck-down region.

Fig. 3 is a schematic diagram of a purpose-built secondary oven with separate preheat and drawing sections. An adjustable iris separates the preheat and drawing sections while additional irises isolate each section from the ambient atmosphere. So as to define a 'tight' hot-zone within the drawing section, impingement heating was employed whereby heated

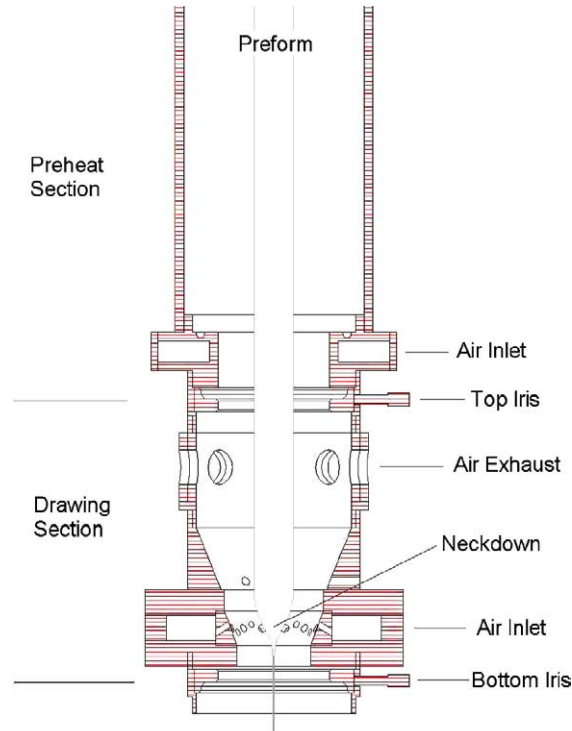


Fig. 3. Schematic diagram of the purpose-built secondary oven showing the preheat and drawing sections and the positions of the two irises, the air exhaust and the neck down region.

nitrogen was directed onto the preform through a ring of closely spaced holes. The nitrogen is pressure regulated and split with the two lines going to the preheat and drawing sections. Each gas flow is monitored and controlled before passing to a separate insulated heater built around a 500 W cartridge heater.

Given the importance of a narrow hot-zone with a minimal radial temperature gradient across the preform, measurements were made to establish the temperature profiles within both the preheat and drawing sections. Within the preheat section, the nitrogen temperature (as measured by a K-type thermocouple) dropped essentially linearly from 105 to 85 °C over a 65 mm length above the iris separating the two sections. The temperature profile in the drawing section was measured by inserting a K-type thermocouple into a 12 mm diameter PMMA rod and drawing this preform to 800 µm fibre. The temperature was logged as a function of time with this data being converted to the profile as a function of position shown in Fig. 4 using the set feed rate (2 mm/min). Note that because of the insulation provided by the PMMA, the profile shown in Fig. 4 probably only provides an acceptable approximation to the nitrogen temperature in the lower half where the preform has begun to thin substantially. The difference in the measured maxima (165 and 172 °C) for the two cases is less than the difference in the inlet temperatures (205 and 230 °C), a fact that is consistent with the higher heat losses expected in the 'hotter' case. More importantly

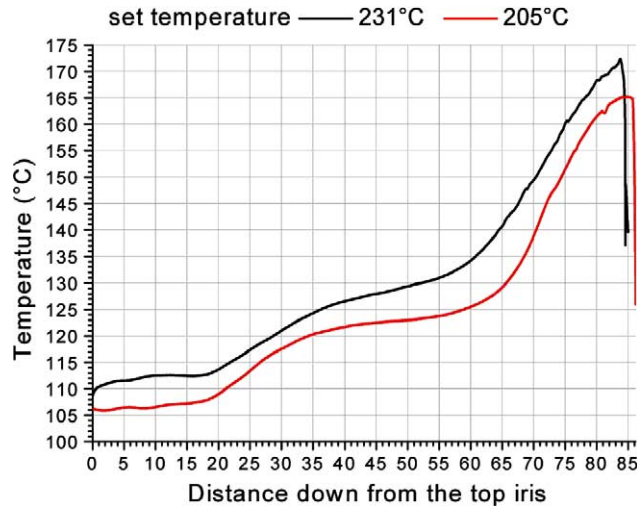


Fig. 4. Temperature profile as measured in the drawing section of the purpose-built secondary oven. The effective hot-zone is reduced to a length of 15–20 mm.

though is the fact that this modest difference in hot-zone temperature results in a more than two-fold difference in tension (145 and 65 g, respectively), emphasising the need for tight hot-zone temperature control in the drawing of mPOFs to limit collapse of the hole structure.

Fig. 4 indicates that the width of the hot-zone in this secondary oven is of the order 15–20 mm. This is a considerable improvement on the 140 mm width estimated for the original oven, in that the scope for material accumulation/depletion as a result of the neck-down region moving is greatly reduced. Indeed as shown in the last row of Table 1, here the measured and predicted fibre diameters are in close agreement.

In addition to redesigning the secondary oven, online monitoring and control of the draw tower (carried out within *LabView*) was also substantially upgraded. The most commonly used control option was to maintain fibre diameter using a feedback controller that adjusted capstan speed on the basis of the calculated deviation between measured and set-point diameter values. In this case, the fibre tension level can be changed by manually adjusting the set-point value on the feedback controller maintaining the temperature of the nitrogen flowing into the drawing section of the oven. An alternative configuration whereby the fibre tension (rather than the fibre diameter) was controlled by adjusting the capstan speed was also implemented but rarely used as it leads to a nonuniform fibre diameter.

3. Material selection

It is important to appreciate that although tight control is necessary when drawing to fibre, successful mPOF fabrication is intimately linked with ‘correct’ material selection. Initial mPOFs were made using a low-cost PMMA commercially available as extruded rod. Although this material was easy to handle at the primary preform stage, its bulk mate-

Table 2
Measured bulk material loss for three types of commercially available PMMA rods

PMMA	Loss (dB/m)
1. Low-cost extruded	4.0
2. High-quality extruded	2.5
3. Low-loss cast	0.67

rial loss as measured using a HeNe laser at a wavelength of 633 nm was high (see Table 2) while it had a tendency to bubble when drawn. This extent of bubbling is consistent with a PMMA that has been prepared by unassisted free-radical polymerisation where the termination step is predominantly by disproportionation. This process leaves two neutral, nonreactive polymer chains, one with a saturated end group (i.e., single bonds), the other with a terminal double bond. The latter unsaturated chain has a greater tendency to depolymerise when heated, leading to the formation of monomer that can vaporise during the drawing process. The measured glass transition temperature (T_g) for this polymer was approximately 95 °C which is at the lower end of the range reported in the literature, a fact that is consistent with the plasticising effect of monomer.

Most of the work reported in this paper used a second source of PMMA, also available as extruded rod. This higher quality material gave very few (if any) bubbles when a preform was drawn to fibre, although its bulk material loss was still quite high. Such a difference in behaviour can be explained by this polymerisation having been carried out in the presence of a chain transfer agent (i.e., an assisted polymerisation), an approach that leads to the ends of all PMMA chains being saturated (i.e., having single bonds). These ends are highly stable and would not be expected to depolymerise when heated up during the drawing process. The T_g for this material was measured as 115 °C, a value consistent with the absence of any significant amount of monomer to act as a plasticiser.

More recently cast PMMA rods have become available, with the second of these materials now being our default choice for any new mPOF design primarily because of its lower bulk transmission loss.

It should be realised that any PMMA choice involves a compromise on material characteristics. For example, our current preference (PMMA 3) is a low-loss cast PMMA which is by far the most difficult to machine being both harder and more brittle than the other options. It might also be noted at this point that the hole structure in the primary preform needs to be thoroughly cleaned out by extensive water flushing (no solvents are used) to remove residual cutting fluid and PMMA micro-swarf from the drilling process. The latter has been identified as a likely contributor to measured scattering losses in the final fibre [9].

4. Quality of mPOF fabricated

One of our clear objectives was to develop a generic fabrication procedure suitable for producing a wide range of mPOFs that met both mechanical and optical ‘quality’ criteria. The optical performance of mPOFs (both numerically simulated and experimentally measured) has been extensively reported in the literature [1–3,10]. This paper is primarily

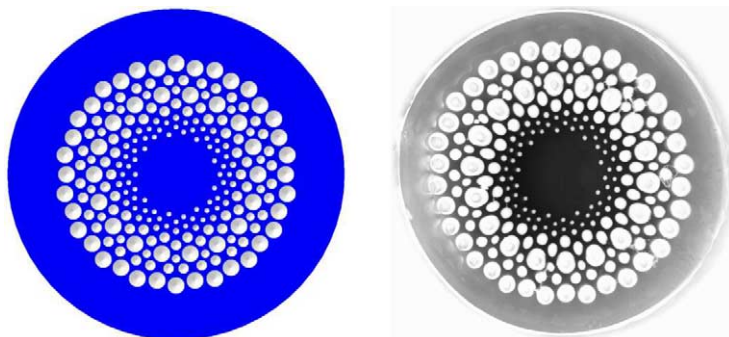


Fig. 5. Left: design of a graded-index mPOF (GImPOF) preform of 80 mm diameter. Right: 220 μm diameter GImPOF as fabricated from such preform.

concerned with two key mechanical criteria, fibre diameter and the extent of hole collapse, both of which impact strongly on the optical performance.

During extensive testing of the secondary oven system, two operational issues emerged that were crucial to the maintenance of tight fibre diameter control. Firstly, the gas flow through the drawing section cannot be so large that turbulent flow patterns cause the developing fibre to vibrate and/or be exposed to highly time dependent heat transfer. Related phenomena have recently been reported for solid polymer fibre drawing [11]. For our system the optimum nitrogen flow to the drawing section was found to be about 2.5 L/min. Secondly, diameter variations increased noticeably if the preform was not accurately centred as it was fed into the oven. As an example, in one case correct centring reduced the standard deviation (about a set fibre diameter of 300 μm) from 33 to 8.7 μm .

A number of options are currently available for making graded-index POF, including interfacial-gel polymerisation [12] and extrusion [13], all of which require somewhat complex fabrication technologies. By comparison, graded-index mPOFs (or GImPOFs) can be made quite readily by varying the hole size as a function of radial position with the azimuthal average of the air–polymer structure providing an acceptable approximation to the requisite quadratic refractive index profile. Fig. 5 shows both the preform hole structure design for a GImPOF [14,15] and a microscope image of the fabricated fibre of 220 μm diameter.

Fig. 6 shows the recorded conditions (fibre tension, draw speed and diameter) corresponding to the drawing of a 37 m length of this GImPOF. The average fibre diameter over the entire length was 200 μm with a standard deviation about this mean of only 1.7 μm . The variations in capstan speed during this draw are due to the feedback control loop responding to variations in preform diameter to keep the fibre diameter constant.

Table 3 gives details of a number of different mPOFs fabricated using our facility. In each case, the measured standard deviation of the fibre diameter about the required value was of the order 2–3 μm over tens of metres. This compares favourably with measurements made on commercial capillary tubing whose (nominal) 250 μm diameter was found to vary by up to ± 25 μm .

The second mechanical quality criterion measured in this work was the extent of the hole collapse between the primary preform and the final fibre. For a range of MPOFs,

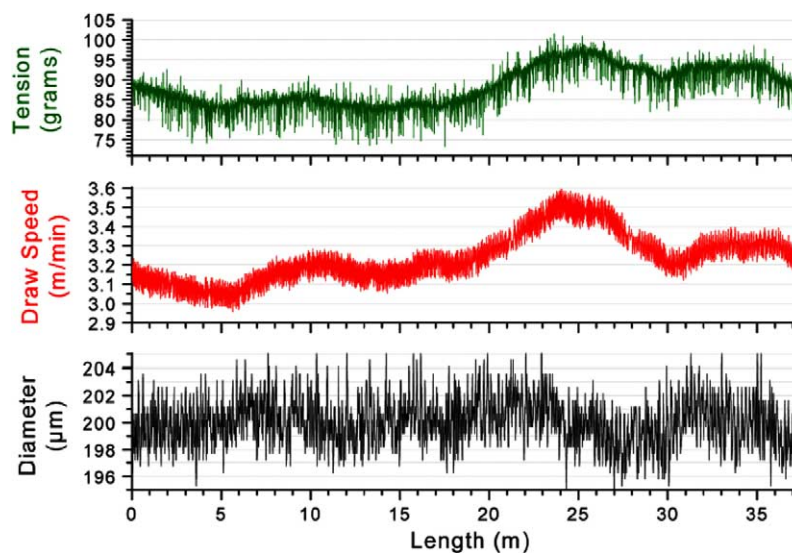


Fig. 6. Drawing conditions such as draw tension, draw speed and diameter as recorded during a draw of GImPOF, using the purpose-built secondary oven. The average fibre diameter over the 37 m fibre length was 200 μm with a standard deviation of 1.7 μm .

Table 3

Data showing the hole size (h) and hole spacing (Λ) in the primary preform, as well as the fibre diameter (d) and the percentage hole collapse in the final drawn fibre (C) for a range of fabricated mPOFs

Fibre type	h (mm)	Λ (mm)	d (μm)	C (%)
Single-mode [1]	4.0	6.0	250	31
Single-mode [14]	1.2	1.7	250	38
Multicore (central holes) [14]	1.2	1.7	200	39
Small-core [8]	1.0	1.2	570	54
Honeycomb [14]	1.2	1.7	230	30
Air-core bandgap [16]	1.0	1.2	500	37
Air-core bandgap [14]	2.0	2.5	160	38
Twin-core [17]	1.2	1.5	200	31

Note that the second and third column relate to preform dimensions whereas the fourth and fifth column refer to fibre dimensions.

Table 3 gives the hole size (h) and hole spacing (Λ) for the primary preform, as well as the fibre diameter (d) and the percentage hole collapse in the final drawn fibre (C), the latter being defined as follows:

$$C = 100 \left(1 - \frac{(h/\Lambda)_{\text{Fibre}}}{(h/\Lambda)_{\text{Preform}}} \right).$$

Average hole size and hole spacing for all drawn fibres (except the small-core fibre) were based on photographs taken using an optical microscope. In the small-core fibre case, more accurate scanning electron microscope measurements of the hole size (0.53 μm) and hole spacing (1.38 μm) of the fibre structure were also taken to allow numerical modelling

to be carried out showing the fibre to be endlessly single-mode [8]. It is worth noting that this fibre required the highest applied tension (180 g) during the draw phase.

Table 3 shows that hole collapse generally varies within the range 30–40% with the exception being the small-core fibre. This level of hole collapse is included as a general rule-of-thumb when designing the primary preform for a new mPOF (see Fig. 1). The issue of hole collapse will be explored more fully in a subsequent paper.

5. Conclusions

The evolution of our fabrication facility clearly demonstrates that a wide range of mPOFs can be readily produced provided that the following conditions are met:

- Heat transfer during both the preform preheating and fibre drawing phases is tightly controlled with the drawing taking place from within a narrow ‘hot-zone.’
- Tension within the fibre is maintained (by adjustment of the temperature within the hot-zone) at a high enough level to prevent unacceptable collapse of the hole structure.
- External fibre diameter is continuously monitored online and controlled by feedback adjustment of the fibre draw speed.

Experimental data indicate that a standard deviation of 2–3 μm in the final fibre diameter and a 30–40% level of hole collapse are representative values over a diverse range of mPOFs fabricated on our facility.

Acknowledgment

The authors thank Barry Reed for his invaluable technical assistance in many facets of this work.

References

- [1] M.A. van Eijkelenborg, M.C.J. Large, A. Argyros, J. Zagari, S. Manos, N.A. Issa, I. Bassett, S.C. Fleming, R.C. McPhedran, C.M. de Sterke, N.A.P. Nicorovici, Microstructured polymer optical fibre, *Opt. Exp.* 9 (2001) 319–327.
- [2] A. Argyros, I.M. Bassett, M.A. van Eijkelenborg, M.C.J. Large, J. Zagari, N.A.P. Nicorovici, R.C. McPhedran, C.M. de Sterke, Ring structures in microstructured polymer optical fibres, *Opt. Exp.* 9 (2001) 813–820.
- [3] M.A. van Eijkelenborg, A. Argyros, G. Barton, I.M. Bassett, M. Fellew, G. Henry, N.A. Issa, M.C.J. Large, S. Manos, W. Padden, L. Poladian, J. Zagari, Recent progress in microstructured polymer optical fibre fabrication and characterisation, *Opt. Fiber Technol.* 9 (2003) 199–209.
- [4] N.P. Bansal, R.H. Doremus, *Handbook of Glass Properties*, New York Academic, 1986.
- [5] H.M. Reeve, A.M. Mescher, A.F. Emery, Steady-state heat transfer and draw force for POF manufacture, in: 12th Int. Conf. on Polymer Optical Fiber (POF 2003), Seattle, USA, 15–17 September, 2003, p. 220.
- [6] S. Wu, Surface and interfacial tensions of polymer melts. II. Poly(methylmethacrylate), poly(*n*-butylmethacrylate), and polystyrene, *J. Phys. Chem.* 74 (1970) 632–638.
- [7] A.D. Fitt, K. Furusawa, T.M. Monro, C.P. Please, Modeling the fabrication of hollow fibers: capillary drawing, *J. Lightwave Technol.* 19 (2001) 1924–1931.

- [8] J. Zagari, G.W. Barton, G. Henry, M.C.J. Large, N.A. Issa, L. Poladian, M.A. van Eijkelenborg, Small-core single-mode microstructured polymer optical fibre with large external diameter, *Opt. Lett.* 29 (2004) 818–820.
- [9] G. Barton, M.A. van Eijkelenborg, G. Henry, N.A. Issa, K.-F. Klein, M.C.J. Large, S. Manos, W. Padden, W. Pok, L. Poladian, Characteristics of multimode microstructured POF performance, in: 12th Int. Conf. on Polymer Optical Fiber (POF 2003), Seattle, USA, 15–17 September, 2003, p. 81.
- [10] N.A. Issa, L. Poladian, Vector wave expansion method for leaky modes of microstructured optical fibres, *J. Lightwave Technol.* 21 (2003) 1005–1012.
- [11] H.M. Reeve, A.M. Mescher, Effect of unsteady natural convection on the diameter of drawn polymer optical fiber, *Opt. Exp.* 11 (2003) 1770–1779.
- [12] M. Sato, T. Ishigure, Y. Koike, Thermally stable high-bandwidth graded-index polymer optical fiber, *J. Lightwave Technol.* 18 (2000) 952–958.
- [13] W.R. White, L.L. Blyler, R. Ratnagiri, M. Park, J.J. Refi, Perfluorinated POF: Out of the lab. into the real world, in: 12th Int. Conf. on Polymer Optical Fiber (POF 2003), Seattle, USA, 15–17 September, 2003, p. 16.
- [14] J. Zagari, The Fabrication of Microstructured Polymer Optical Fibre, Master thesis, Faculty of Engineering, University of Sydney, Australia, 2003.
- [15] M.A. van Eijkelenborg, A. Argyros, A. Bachmann, G. Barton, M.C.J. Large, G. Henry, N.A. Issa, K.F. Klein, H. Poisel, W. Pok, L. Poladian, S. Manos, J. Zagari, Bandwidth and loss measurements of graded-index microstructured polymer optical fibre, *Electron. Lett.* 40 (2004) 592–593.
- [16] M.A. van Eijkelenborg, M.C.J. Large, A. Argyros, I. Bassett, J. Zagari, Photonic bandgap guiding in microstructured polymer optical fibres, in: Int. Quantum Electronics Conf., Moscow, Russia, 22–27 June, 2002, Paper QThH3.
- [17] W. Padden, A. Argyros, S. Manos, M.A. van Eijkelenborg, Coupling in a twin-core microstructured polymer optical fibre, *Appl. Phys. Lett.* 84 (2004) 1689–1691.